J Appl Electrochem (2009) 39:369–375
DOI 10.1007/s10800-008-9680-6

ORIGINAL PAPER

Voltammetric study of the influence of benzotriazole on copper deposition from a sulphuric plating bath

A. C. M. de Moraes · J. L. P. Siqueira · L. L. Barbosa · I. A. Carlos

Received: 23 April 2008 / Accepted: 2 October 2008 / Published online: 18 October 2008

Abstract Copper electrodeposition on to a platinum substrate from an acid sulphate plating bath was investigated with and without the additive benzotriazole (BTAH). In voltammetric experiments, the deposition process is shifted to more negative potentials in the presence of BTAH than in its absence from the bath. Moreover, the current density of the deposition process was higher in the presence of this additive than in its absence. With or without the additive, copper deposition showed features of nucleation in the voltammetric curves. Scanning electronic microscopy (SEM) images showed that copper deposits laid down in the presence of BTAH, for any potential and charge density studied, were smoother than in the absence of this additive. X-ray spectra indicated that the electrodeposits produced in the absence or presence of BTAH were composed of a mixture of copper, copper oxide and platinum oxide and also indicated that in the presence of BTAH, the deposit was less crystalline than in its absence.

Keywords Copper · Benzotriazole · Electrodeposition · Voltammetry · Microscopy · X-ray diffraction

1 Introduction

Sulphuric acid copper electroplating is extensively used in industry, because it is fast, inexpensive, easy to maintain and control, less toxic (cyanide free) and produces deposits of good uniformity, strength and ductility [1–8]. Additives such as benzotriazole (BTAH) have been used in the copper electrodeposition bath and the formation of a film of copper and BTAH has been studied by several groups [4–14] and it has been shown that BTAH is chemisorbed in the form of a Cu(I)-BTA complex at the electrode surface, where it may accept an electron from the cathode and discharge Cu atoms, which are incorporated at the active sites. These experiments have been carried out, in general, with dilute solutions of Cu^{2+} ($\sim 10^{-3}$ M), so that good quality coatings could probably be prepared only with low deposition current densities or potentials. Schimdt et al. [8] investigated copper electrodeposition in the presence of BTAH on to gold substrate and observed that the presence of this additive in the bath led to finer and more homogeneous deposits. Later, that group studied the copper electroplating process, in the absence and presence of several substituted BTAH compounds in the solution, on to a gold/glass substrate [9]. The authors found that in the absence of any additive or presence of 1-(methoxymethyl)-1H-BTAH or methyl-1H-BTAH, the process resulted in rough deposits. However, in the presence of BTAH or *N*-(1H-benzotriazol-1-ylmethyl) formamide, the deposits were smoother. Tantavichet and Pritzker [10] reported that, when BTAH is the only additive present in the solution, it generally has a stronger effect than the plating mode and significantly enhances deposit morphology and surface brightness, in comparison with additive-free solutions. Kim et al. [11] investigated the effect of BTAH on copper electroplating and showed that BTA exhibited both strong suppression and brightening effects by modifying the nucleation and growth steps; electroplating in the presence of BTAH followed a random deposition mechanism rather than a selective or preferential deposition mechanism. Armstrong and Muller [12] studied copper electrodeposition in the presence of BTAH on to a platinum substrate and

A. C. M. de Moraes · J. L. P. Siqueira · L. L. Barbosa · I. A. Carlos (✉)
Departamento de Química, Universidade Federal de São Carlos, CP 676, 13565-905 Sao Carlos, SP, Brazil
e-mail: diac@ufscar.br

observed that the BTAH in the plating bath reduced the size of copper crystallites.

In this investigation, therefore, a systematic electrochemical study of copper electrodeposition on to a platinum electrode in a sulphuric acid plating bath, with and without BTAH, was conducted through cyclic voltammetry. The influence of deposition charge density (q_d) and potential (E_d) on the morphology of the copper deposit, in the absence and in the presence of BTAH, was investigated by SEM. The influence of BTAH on the crystal structure of the copper deposit obtained in selected conditions of charge density and deposition potential was investigated by X-ray diffraction spectroscopy (XRD).

2 Experimental details

All chemicals were analytical grade. Double-distilled water was used throughout. Each electrochemical experiment was performed in a freshly prepared acid bath, containing 0.10 M $CuSO_4$ + 0.1 M H_2SO_4 + 1.0 M Na_2SO_4, with or without the addition of 1.0×10^{-3} M BTAH. A Pt (0.196 cm^2) disk, a Pt plate and a normal calomel electrode (NCE, $E = 0.268$ V), with an appropriate Lugging capillary, were employed as working, auxiliary and reference electrodes, respectively. Immediately prior to the electrochemical measurements, the Pt working electrode was dipped in a concentrated sulphuric–nitric acid solution, then rinsed with water, dipped in an ultrasonic bath for about 1 min and rinsed again. Potentiodynamic curves were recorded with a PARC electrochemical system consisting of a model 173 potentiostat/galvanostat. All experiments were carried out at room temperature (25 °C). Potentiostatic deposits were obtained at 2.5, 5.0 and 7.5 C cm^{-2}. SEM micrographs were taken with a Carl Zeiss model DSM 960 Digital Scanning Microscope with 4 nm resolution. X-ray diffraction patterns were produced with Cu Kα radiation (1.5406 Å), using a Rigaku Rotaflex RU200B X-ray goniometer, in 2θ scanning mode (fixed $\theta = 2^\circ$).

3 Results and discussion

3.1 Electrochemical studies

Figure 1 shows cyclic voltammograms of copper deposition on to a platinum substrate from a sulphuric acid plating bath in the absence (-·-·-) and presence (——) of BTAH at $v = 10$ mV s^{-1}. The main features of these voltammograms are a cathodic peak and an anodic process. It can be seen that in the presence of BTAH the deposition process occurred at a more negative potential (~ -0.55 V) than in its absence (~ -0.25 V). Researchers have proposed [6–13] that BTAH is adsorbed on the substrate and can form a complex with Cu (I), Cu(I)BTAH. Thus, the shift of the deposition potential to more negative values seen in Fig. 1 could be due to adsorption on the platinum substrate of Cu(I)BTAH, which is reduced to Cu.

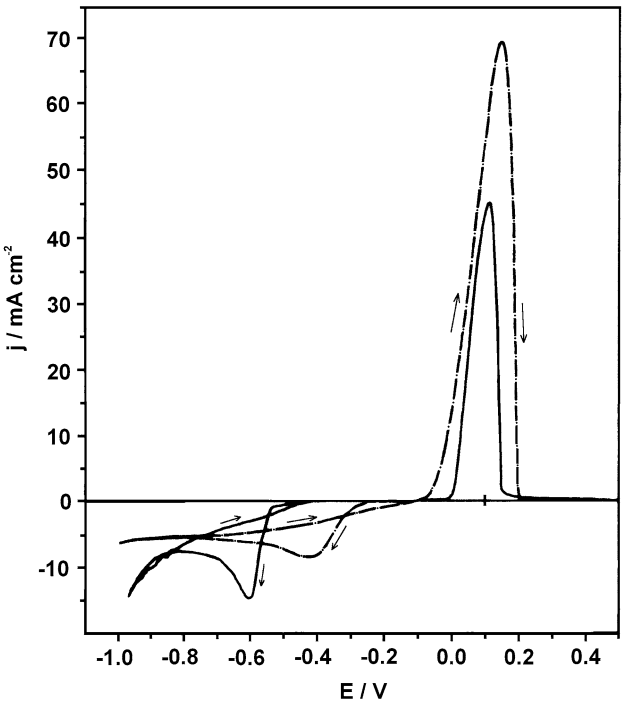

Fig. 1 Voltammetric curves recorded in 0.10 M $CuSO_4$ + 0.10 M H_2SO_4 + 1.0 M Na_2SO_4 baths in the absence (-·-·-) and presence (——) of 1.0×10^{-3} M BTAH from a platinum substrate, at $v = 10$ mV s^{-1}. Potential values were referred to the calomel 0.10 M KCl electrode

Gewirth et al. [9] investigated copper electrodeposition on gold and proposed that Cu nucleates and grows as more copper adatoms are released by reduction of the complex: Cu(I)BTAH(ads) + e^- = Cu (ads) + BTA (ads). The clear current discontinuity observed at ~ -0.55 V (Fig. 1), in the presence of BTAH, is suggestive of nucleation and growth processes [15]. These occurred on top of the thin copper layer formed at ~ -0.45 V, as can be seen better in Fig. 4a. Also, it can be seen in Fig. 1 that the current density of the deposition process is higher in the presence of the additive than in its absence, probably due to the fact that the deposition potential is more negative in the presence of BTAH than in its absence.

The copper dissolution process in the presence or absence of BTAH showed one anodic peak (Fig. 1). The copper dissolution charge density in the presence of BTAH (218.75 mC cm^{-2}) is lower than in its absence (543.75 mC cm^{-2}), due to differences in nucleation potential, which is more negative in the presence of BTAH.

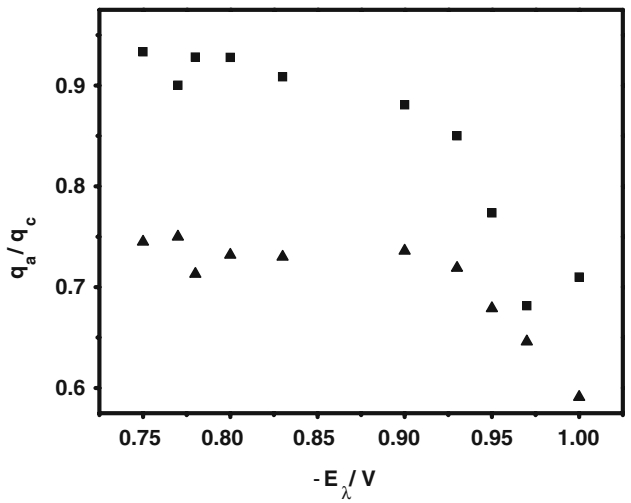

Fig. 2 Dependence of q_a/q_c ratio on the lower switching potential (E_λ) in 0.10 M $CuSO_4$ + 0.10 M H_2SO_4 + 1.0 M Na_2SO_4 solution with 1.0×10^{-3} M BTAH (▲) and without BTAH (■). $v = 10$ mV s^{-1}

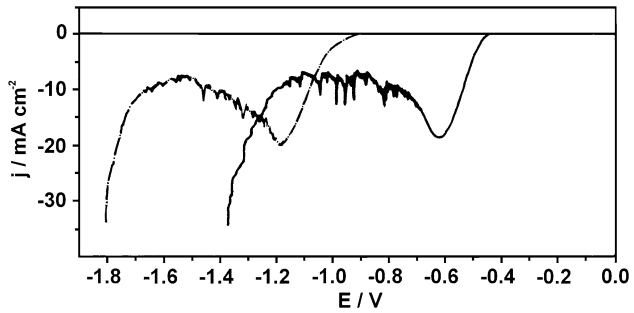

Fig. 3 Hydrogen evolution reaction in 0.1 M H_2SO_4 + 1.0 M Na_2SO_4 + 1.0×10^{-3} M BTAH on platinum (—) and copper (-·-·-) substrates. $v = 10$ mV s^{-1}

Kharafi et al. [16] attributed the remarkable efficiency with which BTAH inhibits the corrosion of copper to its adsorption on the surface (BTAH + Cu = BTAH:Cu) and formation of a protective complex (BTAH + Cu^+ = Cu(I)BTA + H^+). Comparing the initial potentials of the anodic peak in the presence (~−0.10 V) and absence (~0 V) of BTAH, it can be seen that the additive causes a shift of ~100 mV in the positive direction. These findings indicate that adsorption of the additive and so the formation of Cu(I)BTA occurred, corroborating Kharafi et al. [16].

Figure 2 shows a typical plot of the anodic to cathodic charge ratio (q_a/q_c) against the switching potential, E_λ, during potentiodynamic experiments in the absence (■) and in the presence (▲) of BTAH. It can be seen that, for the same range of E_λ, the q_a/q_c without BTAH is higher than when it is present, showing that the contribution of the hydrogen evolution reaction (HER) to the electrodeposition process is more significant in the presence of BTAH. The q_a/q_c ratio is lower than 1, and it decreases significantly when E_λ becomes more negative than −0.90 V. This can be attributed to the HER, as can be seen better in Fig. 3.

Moreover, the q_a/q_c values imply that the increase in the current density, in the presence of BTAH, beyond ~−0.8 V (Fig. 1), is due to the HER occurring in parallel with copper reduction, and this is more significant than in the absence of this additive. For example, the q_a/q_c values obtained at E_λ ~−0.80 V were 0.73 in the presence and 0.93 in the absence of BTAH.

The HER region on platinum (Fig. 3 (—)) and on copper (Fig. 3 (-·-·-)) was investigated further by recording the cathodic voltammograms for these substrates in 0.1 M H_2SO_4 + 1.0 M Na_2SO_4 + 1.0×10^{-3} M BTAH solution. Similar results were obtained in the absence of BTAH. It can be seen in Fig. 3 (—) that the HER on platinum begins at −0.45 V, while on copper this occurs at −0.90 V (Fig. 3 (-·-·-)).

The results in Fig. 2 indicate that the copper deposited on the Pt substrate in the initial moments of the deposition process (at potentials less negative than −0.90 V) probably did not totally cover this substrate, so that the HER proceeds at this stage of the deposition process on the uncovered Pt area, leading to q_a/q_c ratio lower than 1. Also, comparing Fig. 1 (—) and Fig. 3 (-·-·-), it may be noted that at E more negative than −0.90 V, the HER on copper is activation-controlled, while the copper deposition (Fig. 1(—)) is mass-transport controlled and the q_a/q_c ratio (Fig. 2) falls significantly.

The variable features of the deposition and dissolution processes are shown in Fig. 4 as functions of switching potential (E_λ), where the sweep is reversed. At ~E_λ = − 0.50 V (Fig. 4a), a cathodic process (q_c = 6.12 mC cm^{-2}) is seen, due to deposition of some copper crystallites in parallel with the HER (which was visible to the naked eye). In the anodic scan, a peak can be seen (~−0.40 V) for the oxidation of molecular hydrogen (q_a = 0.234 mC cm^{-2}), which is clearer in the inset in Fig. 4a. Moreover, in Fig. 4a there is another anodic peak at ~+0.1 V due to oxidation of the copper crystallites (0.345 mC cm^{-2}). In addition, Fig. 3 and the Fig. 4a) inset show that the HER on Pt in the presence of BTAH begins at ~−0.45 V and, considering that the reversible potential of the system $Pt/H_3O^+/H_2$, at pH 1, is ~−0.33 V versus NCE, there is an overpotential for this reaction of 0.120 V. This result indicates adsorption of BTAH followed by formation of the copper complex. It must be stressed that, at ~E_λ = −0.50 V (Fig. 4a), deposition of some copper crystallites occurred, which dissolved at ~+0.1 V.

When the sweep was extended to more cathodic potentials, such as −0.80 V (Fig. 4b), a sudden rise in the current and crossover were observed, indicating that is

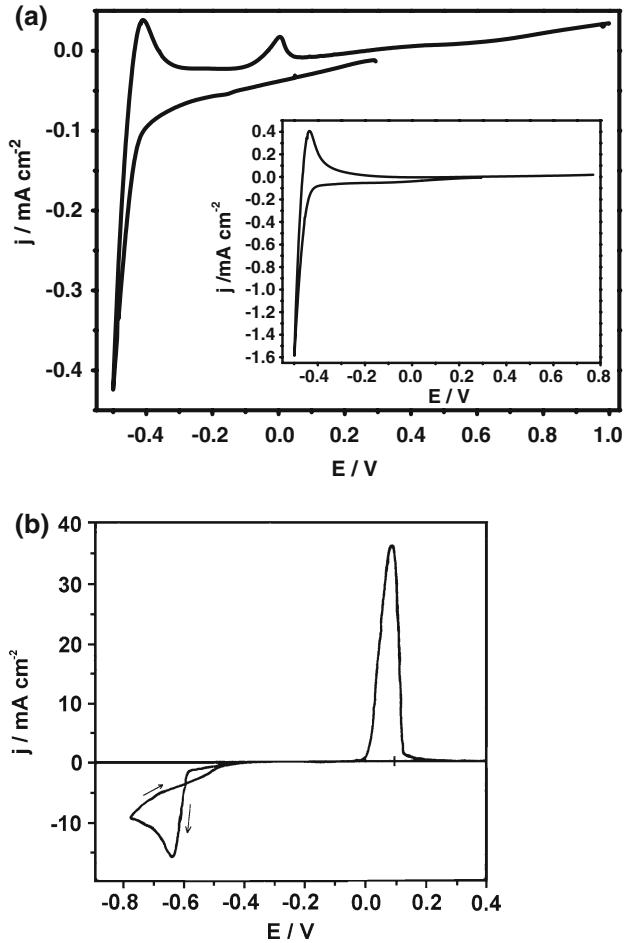

Fig. 4 Reversed sweep voltammograms obtained from 0.10 M $CuSO_4$ + 0.10 M H_2SO_4 + 1.0 M Na_2SO_4 + 1.0 × 10^{-3} M BTAH. Sweep direction reversed at switching potential (E_λ): **a** −0.50 V and **b** −0.80 V. Inset: 0.10 M H_2SO_4 + 1.0 M Na_2SO_4 + 1.0 × 10^{-3} M BTAH. v = 10 mV s^{-1}

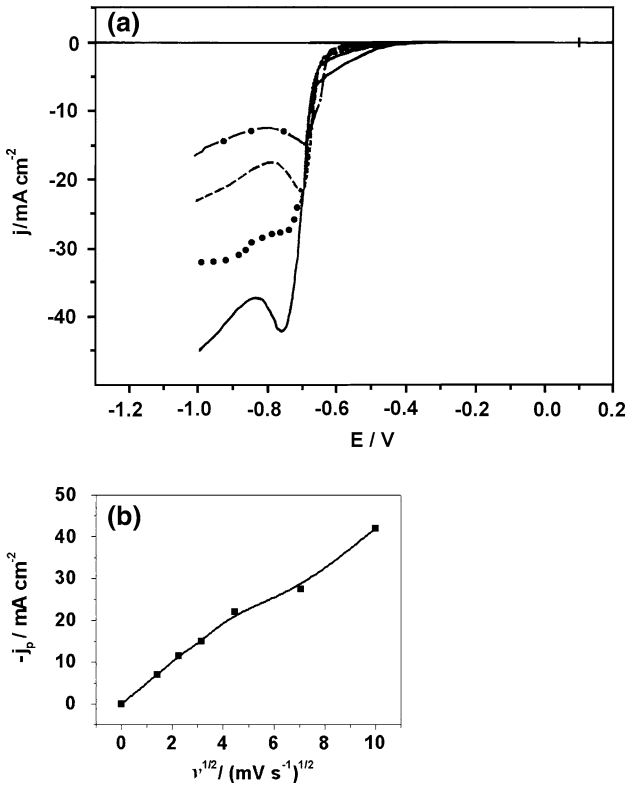

Fig. 5 **a** Deposition voltammograms of the bath 0.1 M $CuSO_4$ + 0.1 M H_2SO_4 + 1.0 M Na_2SO_4 + 1.0 × 10^{-3} M BTAH, carried out at v: 10 (–·–·–); 20 (—); 50 (•••) and 100 (—) mV s^{-1}; **b** Graph of peak current versus square root of sweep rate. Potential values were referred to the calomel 0.1 M KCl electrode

likely that the deposition process occurred by nucleation [15]. These results corroborate those recorded in Fig. 1. Moreover, it can be seen that in the anodic scan (Fig. 4b) there is a peak at ∼+0.10 V, due to oxidation of Cu, but no oxidation peak for molecular hydrogen.

Figure 5a shows copper deposition voltammograms at various sweep rates (v). It can be observed that the peak current density increases with the sweep rate. The peak current for reduction of Cu^{2+} species is modelled by Eq. 1, which includes the reduction of soluble species to form insoluble species [17, 18]:

$$j_p = 367n^{3/2}AC_0D^{1/2}v^{1/2} \quad (1)$$

Figure 5b shows that the peak current density (j_p) increases with $v^{1/2}$, but is not quite linear, suggesting that the Cu electrodeposition process may be controlled by charge transfer and mass transport in this region [19].

3.2 Scanning electronic microscopy

Figures 6a–f and 7a–f show SEM micrographs of copper deposited from the copper plating bath at various deposition potentials and charge densities, in the presence and in the absence of BTAH. Comparing these sets of micrographs, it can be observed that the copper deposits completely covered the substrates in all cases, but had dissimilar morphologies. Note that the lines in some of the micrographs in these figures are due to polishing of the Pt substrates. It can be seen in Figs. 6b, d, f and 7b, d, f that the size of copper crystallites obtained in the absence of BTAH increased with increasing charge density from 2.5 to 7.5 C cm^{-2} and that this increase is more significant at −0.80 V (Fig. 7b, d, f). The increasing size of crystallites at more negative deposition potential and higher charge density indicates that the growth rate of copper crystallites increases faster than the nucleation rate. In the presence of BTAH (Figs. 6a, c, e and 7a, c, e), the copper deposits obtained at both potentials and at all the charge densities showed refining of copper crystallites. These results corroborate those obtained by Muller and Armstrong [12] and Gewirth et al. [8, 9].

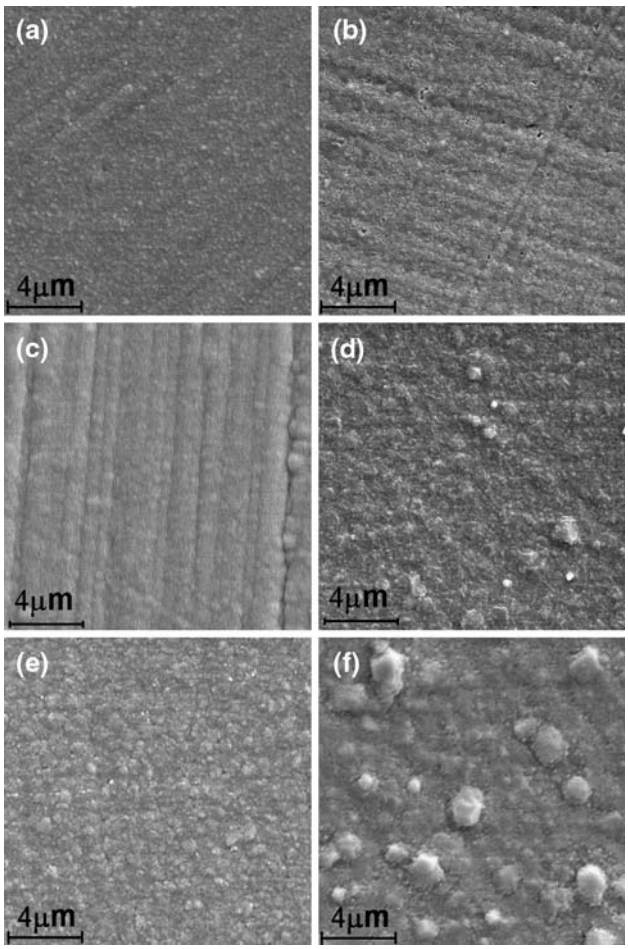

Fig. 6 SEM micrographs of deposits obtained chronoamperometrically from 0.1 M $CuSO_4$ + 0.1 M H_2SO_4 + 1.0 M Na_2SO_4 plating bath on to platinum substrate at −0.55 V, in the presence of 1.0×10^{-3} M BTAH and at a q_d of **a** 2.5 C cm^{-2}; **c** 5.0 C cm^{-2} and **e** 7.5 C cm^{-2} and in the absence of BTAH and at a q_d of **b** 2.5 C cm^{-2}; **d** 5.0 C cm^{-2} and **f** 7.5 C cm^{-2} (5,000×). Potential values were referred to the calomel 0.10 M KCl electrode

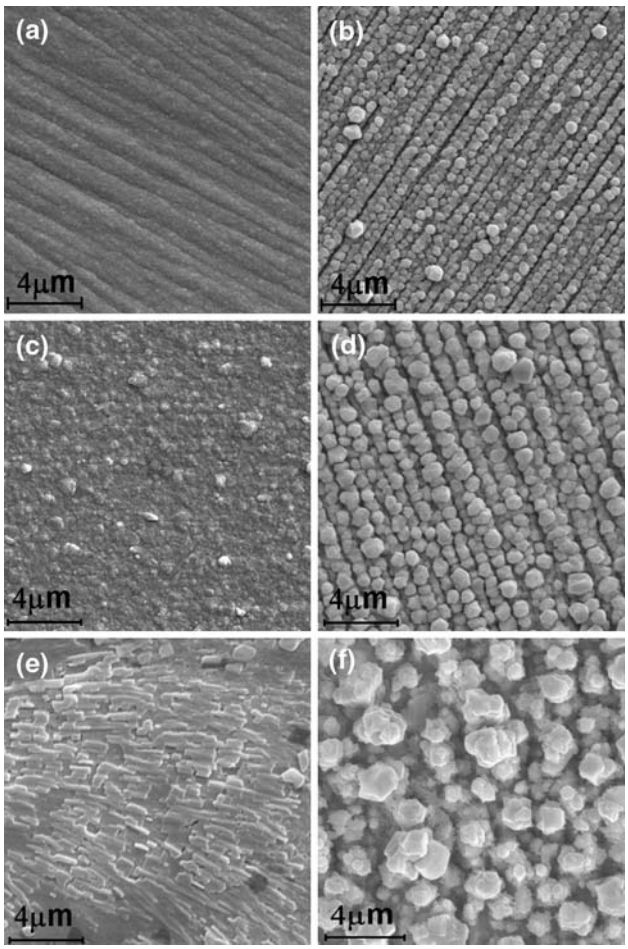

Fig. 7 SEM micrographs of deposits obtained chronoamperometrically from 0.1 M $CuSO_4$ + 0.1 M H_2SO_4 + 1.0 M Na_2SO_4 plating bath on to platinum substrate at −0.80 V, in the presence of 1.0×10^{-3} M BTAH and at a q_d of **a** 2.5 C cm^{-2}, **c** 5.0 C cm^{-2} and **e** 7.5 C cm^{-2} and in the absence of BTAH and at a q_d of **b** 2.5 C cm^{-2}; **d** 5.0 C cm^{-2} and **f** 7.5 C cm^{-2} (5,000×). Potential values were referred to the calomel 0.1 M KCl electrode

The copper plating bath thus proved promising, not only for the good characteristics of the copper deposits, but also because this system contains the additive at a concentration of low toxicity [20], which can be treated with Fenton's reagent (Fe^{2+}/H_2O_2) [21].

3.3 X-ray analysis of the copper deposits

Figure 8a and b shows X-ray diffraction patterns of deposits obtained from a solution containing 0.10 M $CuSO_4$ + 0.10 M H_2SO_4 + 1.0 M Na_2SO_4 in the presence and in the absence of 1.0×10^{-3} M BTAH, respectively, at a deposition potential (E_d) of −0.80 V and $q_d = 5$ C cm^{-2}. These deposition conditions (E_d and an intermediate q_d) were chosen since the morphological differences between the copper deposits obtained in the presence and in the absence of BTAH were more significant than those obtained at −0.55 V and $q_d = 5$ C cm^{-2}. Thus, the X-ray analysis was performed to discover whether these morphological differences were due to structural differences of copper deposits.

The observed crystallographic distances, *d* (hkl), and expected values from phases described in JCPDS [22] are in Table 1.

The diffractograms of the deposits obtained in the absence and in the presence of BTAH were similar. The results obtained without the additive (Fig. 8b) indicate a mixture of copper, with the following reflections: (1 1 1), (2 2 0), (2 0 0), (2 2 2), (3 1 1), and Pt_3O_4 [(2 0 0), (3 1 0)] and $CuPt_3O_6$ [(3 1 1), (3 2 1)], while the diffractogram obtained with BTAH in the bath (Fig. 8a) shows a deposit formed of: Cu [(1 1 1), (2 2 0), (2 2 2), (3 1 1)], PtO (2 2 0), Pt_3O_4 (3 2 1) and $Cu_{64}O$ [(4 4 0), (4 0 12)]. The presence of copper oxides in the bulk deposits is probably due to the

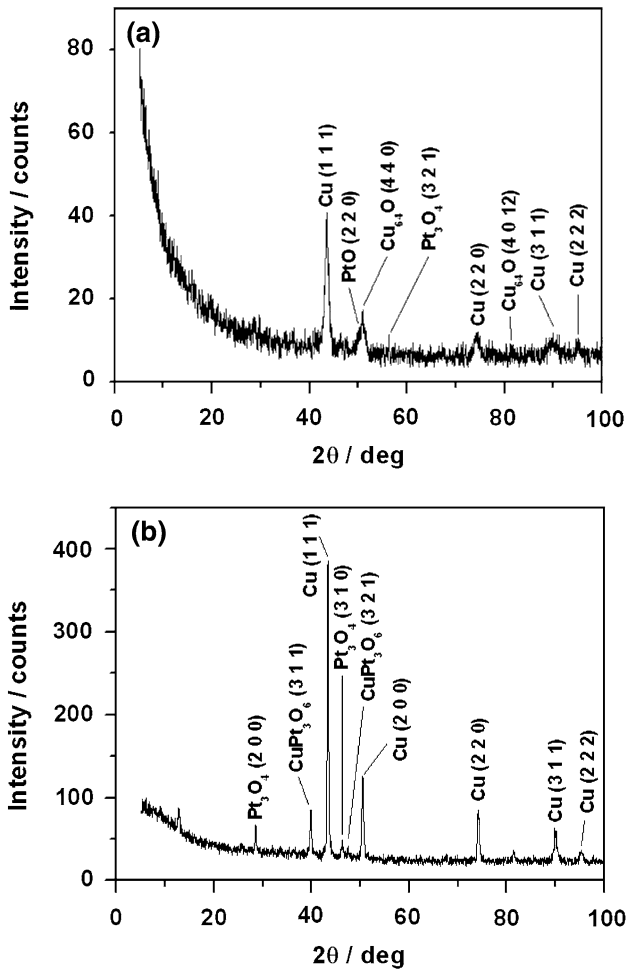

Fig. 8 X-ray diffraction patterns of deposits obtained from 0.1 M $CuSO_4$ + 0.1 M H_2SO_4 + 1.0 M Na_2SO_4 plating bath on to platinum substrate in: **a** presence and **b** absence of 1.0×10^{-3} M BTAH, at −0.80 V and $q_d = 5.0$ C cm^{-2}, on to Pt substrate. Potential values were referred to the calomel 0.1 M KCl electrode

HER on the deposit leading to an increase in the interfacial pH and formation of oxides during the reduction process.

Comparing Fig. 8a and b, it can be seen that XRD peaks in the presence of BTAH were more broadened than in the absence of this additive, indicating that in the first case the deposit is less crystalline than that obtained in the absence of BTAH. Thus, the morphological differences observed in the deposits obtained at −0.80 V and $q_d = 5$ C cm^{-2} (Fig. 7c, d) are due a difference in degree of crystallinity.

4 Conclusion

Copper electrodeposits were successfully obtained from a sulphuric acid bath containing BTAH. The addition of BTAH to the copper plating bath shifted the reduction process to more negative potentials. The copper electrodeposition may be controlled by charge transfer and mass transport in the region of the cathodic peak**.** The significant fall in the q_a/q_c ratio as deposition potential becomes more negative than −0.90 V is attributed to HER occurring on the deposited copper in parallel with copper reduction. SEM analysis showed that the presence of BTAH in the plating bath improved the morphological characteristics of copper deposits obtained at two different deposition potentials and various charge densities, in that they were smoother than in the absence of this additive. The reduction of grain size was due to the more negative deposition potential required in the presence of BTAH.

X-ray analysis of the deposits obtained at −0.80 V and 5 C cm^{-2} indicated that in the presence of BTAH the deposit was less crystalline than in its absence.

Table 1 Observed interplanar distances, d (hkl), of X-ray patterns of copper deposits obtained at $E_d = -0.80$ V and $q_d = 5$ C cm^{-2}, from bath 0.10 M $CuSO_4$ + 0.10 M H_2SO_4 + 1.0 M Na_2SO_4 in: (a) presence of 1.0×10^{-3} M BTAH and (b) absence of BTAH

d_1(hkl) (a)	d_2(hkl) (b)	d_{exp}(Cu)	d_{exp}($Cu_{64}O$)	d_{exp} (Pt_3O_4)	d_{exp}(PtO)	d_{exp} ($CuPt_3O_6$)
	3.1228 (15)			3.113 (88)		
	2.208 (21)					2.253 (20)
2.0796 (49)	2.0860 (100)	2.088 (100)				
	1.8894 (8)					1.899 (8)
1.8091 (13)	1.8071 (33)	1.808 (46)				
1.8186 (23)					1.820 (90)	
1.7938 (25)			1.7915 (24)			
1.6863 (14)	1.6648 (7)			1.664 (13)		
1.2889 (11)	1.2782 (20)	1.278 (20)				
1.1779 (13)			1.1807 (6.2)			
1.0903 (16)	1.089 (17)	1.090 (17)				

The expected values are from JCPDS [18]. Potential values were referred to the calomel 0.1 M KCl electrode

d_{obs}:d_1(hkl) and d_2(hkl)

Acknowledgement Financial support from the Brazilian research foundation FAPESP (Proc. 04/14142-2; 06/51249-5) is gratefully acknowledged.

References

1. Reid JD, David AP (1987) J Electrochem Soc 134:1389
2. Parthasaradhy NV (1989) Practical electroplating handbook. Prentice Hall, New Jersey
3. Lowenheim FA (1974) Modern electroplating, 2nd edn, New York
4. Yoon S, Schwartz M, Nobe K (1994) Plat Surf Finish 10:65
5. Farndon EE, Walsh FC, Campbell SA (1995) J Appl Electrochem 15:574
6. Sheshadri S (1975) J Electroanal Chem Interface Electrochem 61:353
7. Scendo M, Malysko J (2000) J Electrochem Soc 147:1758
8. Schmidt WU, Alkire RC, Gewirth AA (1996) J Electrochem Soc 143:3122
9. Leung TYB, Kang M, Corry BF, Gewirth AA (2000) J Electrochem Soc 147:3326
10. Tantavichet N, Pritzker M (2006) J Appl Electrochem 36:1572
11. Kim JJ, Kim SK, Bae JU (2002) Thin Solid Films 415:101
12. Armstrong MJ, Muller RH (1991) J Electrochem Soc 138:2303
13. Kester JJ, Furtak TE, Bevolo AJ (1982) J Electrochem Soc 129:1716
14. Vogt MR, Polewska W, Magnussen OM, Behm RJ (1997) J Electrochem Soc 144:113
15. Fletcher S, Halliday CS, Gates D, Westcott M, Lwin T, Nelson G (1983) J Electroanal Chem 159:267
16. Kharafi FM, Abdullah AM, Ateya BG (2007) J Appl Electrochem 37:1177
17. Berzins T, Delahay P (1953) J Am Chem Soc 75:555
18. Mamantov G, Manning DL, Dale JM (1965) J Electroanal Chem 9:253
19. Siqueira JLP, Carlos IA (2007) J P Sources 169:361
20. http://www.epa.gov, as on 20 September 2005
21. Harris DC (1996) Quantitative chemical analysis. W H Freeman and Company, New York, p 768
22. Joint Committee on Powder Diffraction Standards (JCPDS) in International Centre for Diffraction Data (2000). Powder diffraction file—PDF-2. Database sets 1–49. ICDD, Pennsylvania (CD-ROM)